

The effect of pressure on phase selection during nucleation in undercooled bismuth

W. Yoon

University of Wisconsin-Madison, Department of Metallurgical and Mineral Engineering, Madison, Wisconsin 53706

J. S. Paik

Korea Standards Research Institute, Taejeon, Korea

D. LaCourt

General Electric Co., Lynn, Massachusetts 01901

J. H. Perepezko

University of Wisconsin-Madison, Department of Metallurgical and Mineral Engineering, Madison, Wisconsin 53706

(Received 19 May 1986; accepted for publication 4 August 1986)

At a sufficiently large liquid undercooling, the solidification of fine Bi droplet samples at ambient pressure yields a metastable phase instead of the stable structure. The metastable Bi phase is observed to melt at 174 °C at ambient pressure. Thermal analysis measurements on droplet samples subjected to hydrostatic pressures ranging up to 400 MPa demonstrate that the melting temperature of the metastable Bi phase increases by 20.8 K/GPa with pressure, while that of the stable Bi phase decreases by 38.8 K/GPa. The trend of the measured melting temperature of the metastable Bi phase joins smoothly to the melting curve of the Bi(II) high-pressure phase. Differential scanning-calorimetry measurements on a liquid Bi droplet sample at undercoolings up to 220 °C support the identification of the metastable Bi phase as the Bi(II) high-pressure phase with a heat of fusion 5.98 kJ/g-at. A shift of the nucleation temperature under pressure, which follows the trend of the melting temperature, characterizes the nucleation onset of both Bi(I) and Bi(II) phases and provides information on the kinetic competition controlling phase selection.

I. INTRODUCTION

Since the early work of Bridgman in 1935,¹ in which four high-pressure polymorphs were proposed for Bi over a pressure range of up to 5 GPa, the elevated pressure-induced phase transitions of Bi have been studied extensively and used widely for pressure calibration points above room temperature by many investigators. With a pressure range extending to 14 GPa and for a temperature range from melting down to 30 K, nine high-pressure polymorphs of Bi have been reported to date.² Figure 1 shows the equilibrium pressure-temperature phase diagram of Bi up to 5 GPa with the various polymorphs labelled mainly in accord with Bridgman's nomenclature.

Despite considerable interest in bismuth at high pressures, the crystal structure is known for three of the polymorphs: Bi(I), Bi(II), and Bi(VI). The Bi(I) phase is stable at ambient conditions with a rhombohedral (2 atoms per unit cell) structure,³ Bi(II) is base centered monoclinic with four atoms per unit cell with cell parameters of $a = 0.6674$ nm, $b = 0.6117$ nm, $c = 0.3304$ nm, and $\beta = 110.33^\circ$ at 2.6 GPa and 30 °C,⁴ and Bi(VI) is base-centered cubic with two atoms per unit cell and a cell parameter of $a = 0.3800$ nm at 9 GPa and room temperature.

Since the driving free energy for the solidification of a phase is related directly to the amount of undercooling below the melting temperature of the phase, a high level of undercooling can expand the product selection involved in

nucleation to an increased variety of types of structures.⁵ At increasing levels of undercooling, additional features may appear during thermal cycling through crystallization and melting. In fact, in a recent undercooling study of pure Bi,⁶ a metastable Bi phase has been shown to compete successfully with the equilibrium Bi(I) phase. As a result, it has been possible to examine Bi in order to study in more detail the effect of pressure on the liquid undercooling behavior and the phase selection kinetics during nucleation.

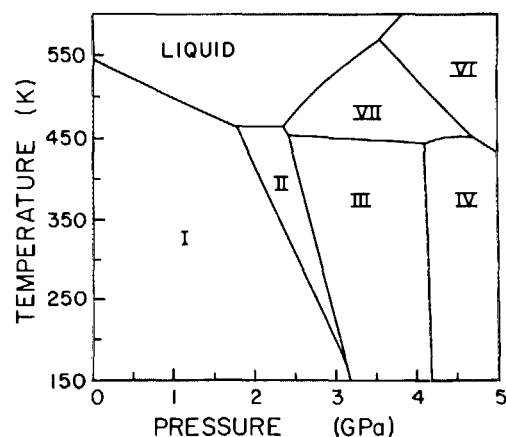


FIG. 1. The pressure-temperature phase diagram for Bi (from Ref. 2).

II. EXPERIMENTAL PROCEDURE

An effective experimental approach that may be applied to yield a large undercooling before the initiation of solidification involves the slow cooling of a dispersion of stabilized fine, liquid metal droplets.^{7,8} By dispersing a high-purity liquid sample into a large number of small drops with diameters below $20\ \mu\text{m}$ within a suitable medium, only a small fraction of the drops may contain potent nucleants. If droplet independence and separation can be maintained by surface coating treatments without introducing potent catalytic sites, then the effects of any internal nucleants can be restricted to a minor fraction of the droplet population so that the majority of the droplets will display a large undercooling. From the observed undercooling behavior of droplet samples,⁹ it is apparent that the largest undercooling range requires a sample with a fine, narrow size distribution and a uniform, non-catalytic surface coating.

The Bi metal used in this investigation was of 99.999 % purity. A mixture of molten Bi, an organic carrier fluid, and surfactant additions was sheared at 30,000 rpm to produce an emulsion. The final droplet size was in the range of $1\text{--}20\ \mu\text{m}$.¹⁰ The melting and crystallization behaviors of droplet samples at ambient pressure were studied with differential thermal analysis (DTA) and differential scanning calorimetry (DSC).

The pressure-generating system with an attached high-pressure DTA block for pressure work is shown in Fig 2. Pressures up to about 0.4 GPa were produced through an intensifier driven by an air pump, which was initiated by a hand pump. The high-pressure DTA block is illustrated schematically in Fig. 3. The details of experimental apparatus and procedures have been presented elsewhere.¹¹

III. RESULTS

A. Droplet undercooling behavior

The droplet dispersal operation isolates the sample from interaction with the container walls, but substitutes the emulsion stabilizing surface coating, which is required to maintain droplet independence. When internal nucleants are effectively isolated into a small fraction of a droplet emulsion, the droplet surface coating is believed to be a limiting factor for the undercooling. In fact, by varying the drop-

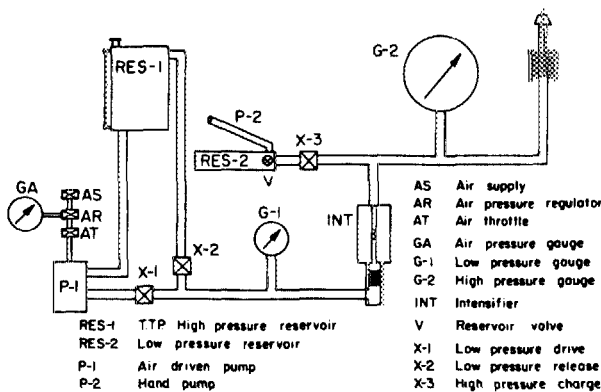


FIG. 2. Schematic representation of the pressure-generating system.

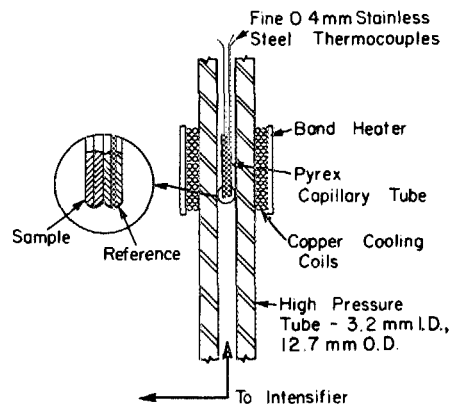


FIG. 3. Schematic representation of DTA block of the pressure equipment.

let surface treatments, different levels of undercooling have been attained as illustrated in Fig. 4.⁶ In each case the droplet emulsion is characterized by a narrow size distribution with an average size of less than $10\ \mu\text{m}$. At the deepest undercooling, the sample behavior shown in Fig. 4(c) exhibits an extra endotherm at $174\ ^\circ\text{C}$ in addition to the equilibrium melting peak at $271\ ^\circ\text{C}$ upon heating. The corresponding cooling trace in Fig. 4(c) also shows an extra thermal signal. It should be noted that a typical DTA sample contains on the

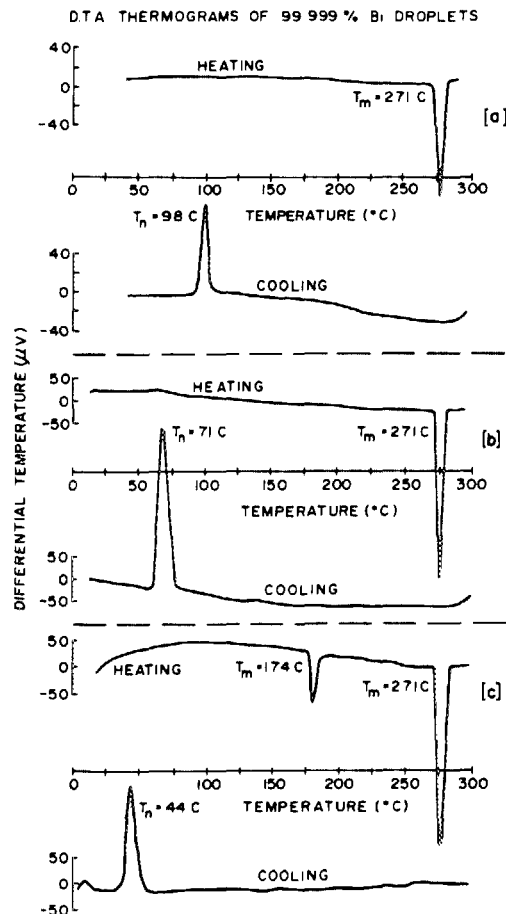


FIG. 4. DTA thermograms for Bi droplets. Different surfactant treatments have yielded changes in the maximum undercooling to nucleation.

order of about 10^6 separate droplets. Due to the surface coating of the droplets, each droplet is independent in its behavior. The thermal signals recorded during DTA therefore represent the summation of events in a statistically significant number of droplets. At the same time due to variations in droplet coating, different droplets may display different kinetic behavior. As a result, although the main crystallization exotherm in Fig. 4(c) at 41 °C may involve metastable phase formation, one droplet fraction can undergo a solid state change subsequently to the equilibrium phase and melt at 271 °C, while another fraction can retain the metastable structure and melt at 174 °C.

The various thermal signals which may be associated with nucleation, decomposition, or melting of the metastable phase have been examined in more detail by performing controlled thermal cycling treatments as illustrated in Fig. 5. In the first heating from the room temperature, the emulsified sample exhibits two endotherms as described before. However, the second heating trace, which was taken after cooling to -10 °C does not show the 174 °C endotherm. Cooling to below room temperature appears to result in a decomposition of the metastable phase which melts at 174 °C. In fact, the reappearance of the metastable phase endotherm when cooling is stopped just after the first exotherm confirms that the second exotherm at the lower temperature actually represents the decomposition of the metastable phase. Moreover, cooling a sample just after the metastable endotherm is reached on heating reproduces the nucleation and the decomposition behavior of the Bi emulsion sample. The thermodynamics of the decomposition of the metastable phase at low temperature will be discussed later. Regardless of the cooling treatment, the metastable phase could not be preserved at room temperature for an extended period of time for x-ray diffraction structural analysis.

B. Pressure-modified undercooling behavior

The pressure dependence of the undercooling, nucleation, and melting temperatures of Bi emulsion samples has

been monitored by a high-pressure DTA system. Several pressure thermograms for Bi emulsion samples are shown in Fig. 6. At ambient pressure, the liquid sample nucleates at 56 °C during cooling and displays the metastable phase melting peak at 174 °C during heating. As pressure increases, the onset temperature of the metastable endotherm as well as the amount of metastable phase, which can be evaluated by the area within the peak, increase steadily. On the other hand, the melting temperature of Bi(I) decreases with increasing pressure. However, the pressure dependence of the nucleation temperature is not monotonic. In the low-pressure range below about 100 MPa, the nucleation temperature decreases as pressure increases during cooling (Fig. 6, curves 1–2), but in the high-pressure range, the nucleation temperature stops decreasing (Fig. 6, curves 2–3) and then begins increasing (Fig. 6, curves 3–4). The shape of the nucleation peak also changes to become sharper with increasing pressure.

As expected, the equilibrium melting temperature decreases as pressure increases by -38.8 K/GPa, while the metastable phase melting temperature increases with pressure by 20.8 K/GPa. The dT/dP value of the Bi(I) melting agrees well not only with the value of -36 K/GPa calculated from the Clausius–Clapeyron relation, but also with Bridgman's experimental value of -38 K/GPa.¹

A Bi emulsion sample which was treated to nucleate at 79 °C at ambient pressure was also pressurized. The sample did not show any indication for nucleation of the metastable phase for pressures up to 400 MPa, but it did show a shift of the Bi(I) nucleation by -29 K/GPa and melting temperature change by the same dT/dP value obtained on the sample shown in Fig. 6 with changing pressure.

The experimental pressure dependence of thermal events for both of the Bi emulsion samples is superimposed on a portion of the P - T diagram for pure Bi in Fig. 7. The melting behavior of the equilibrium Bi(I) phase shows good consistency with the previous data.^{1,12} The melting points of the metastable phase observed in this work can be joined

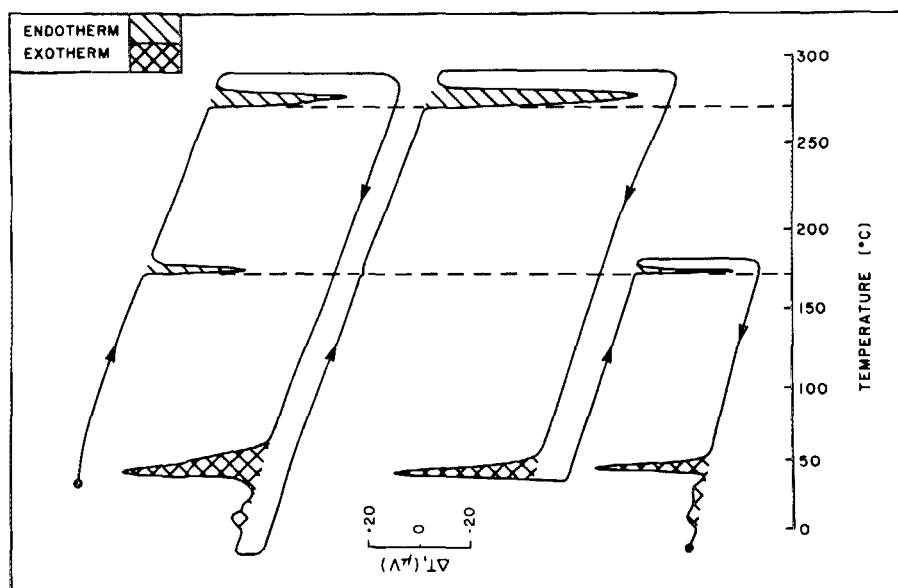


FIG. 5. DTA thermograms for Bi droplets at maximum undercooling. Thermal cycles reveal melting of a metastable phase at 174 °C.

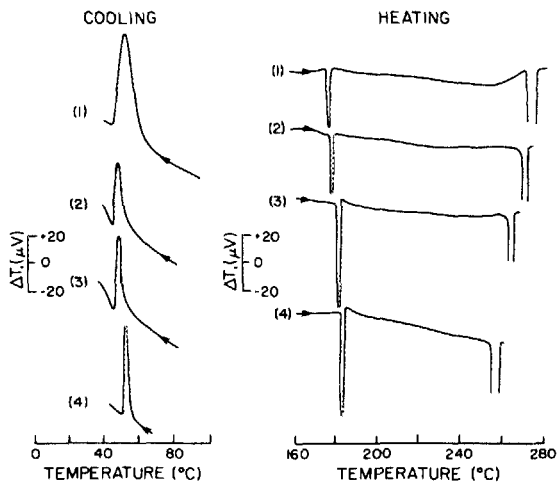


FIG. 6. Pressure thermograms for a Bi droplet sample. (1) 41 MPa, (2) 114 MPa, (3) 276 MPa, (4) 403 MPa.

smoothly by extrapolation with the high-pressure equilibrium melting curve of Bi(II) obtained by Klement *et al.*¹² The Bi(II) melting curve based on DTA measurements was reported to be essentially flat at about 191 °C over the limited pressure range of 1.7–2.4 GPa where Bi(II) is stable. Since the compressibility of liquids is generally larger than that for solids, a convex curve was used for extrapolation of the Bi(II) melting curve to the high-pressure range. This extra-

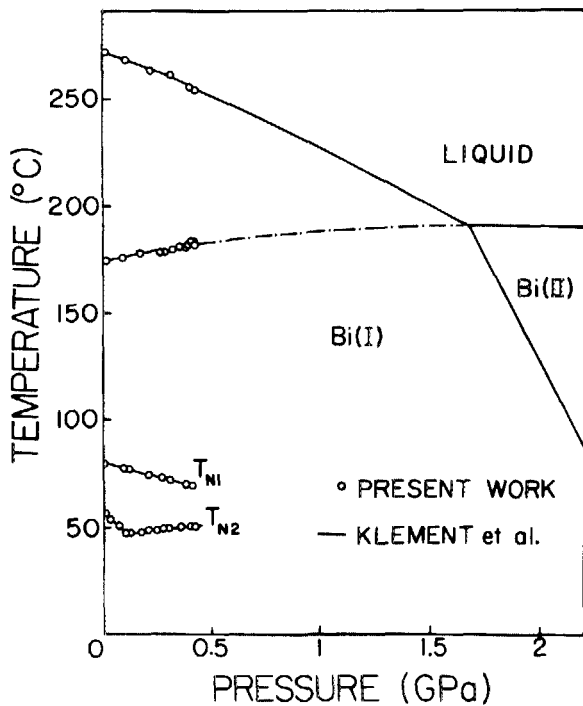


FIG. 7. The pressure-temperature phase diagram for Bi with the experimental data of droplet nucleation and melting behavior. T_{n1} is the trend of nucleation temperature of the droplet sample which solidified at 79 °C at ambient pressure. T_{n2} is the trend of nucleation temperature of the droplet sample which solidified at 56 °C at ambient pressure.

polution is most consistent with the measured stable Bi(II) melting due to Klement *et al.*¹² shown in Fig. 7 and indicates that the observed metastable phase is Bi(II).

C. Thermodynamic evaluation

The heat of fusion ΔH_m of the Bi(II) phase may be determined from experimental data of the pressure dependence of the melting temperature dT/dP on the basis of the Clausius–Clapeyron equation

$$\frac{dT}{dP} = \frac{T_m \Delta V}{\Delta H_m}, \quad (1)$$

where ΔV is the volume change upon melting of Bi(II) and T_m is the melting temperature. However, an accurate ΔV value at ambient pressure and at the melting temperature of Bi(II) is not known. From previous high-pressure experimental results,^{1,12} ΔV values over the pressure range of 1.7–2.6 GPa can be obtained, but these values are small and too uncertain for an accurate ΔH_m determination. Furthermore, the compressibility of the Bi(II) phase is not known exactly. The heat of fusion of the Bi(II) phase, therefore, was measured by performing an independent calorimetric measurement by a DSC method.

During the heating of an emulsion sample, which exhibited a maximum undercooling $\Delta T = 227$ °C, two endotherms were recorded as noted in Fig. 5 and the heat associated with each endotherm was measured separately. The parameters Q_1 and Q_2 indicate the heat involved in the metastable and the equilibrium melting event, respectively, and W_1 and W_2 are the mass of the droplet sample in each event in the metastable and the equilibrium phases, respectively. By cooling the same sample from the completely liquid state through freezing to below the decomposition temperature of Bi(II) phase, the metastable phase formed during crystallization was completely decomposed to the equilibrium Bi(I) phase. The sample was then heated to above the equilibrium melting temperature to measure the total heat Q_3 involved during melting of Bi(I). The mass involved in the melting of the equilibrium sample is symbolized as W_3 . The heats involved in the endotherms of the emulsified sample can be represented as

$$\begin{aligned} Q_1 &= \Delta H_m W_1, \\ Q_2 &= \Delta H_e W_2, \end{aligned} \quad (2)$$

where ΔH_m is the heat of fusion of the metastable phase and ΔH_e is fusion of the equilibrium phase. Also, the heat based on the endotherm of the decomposed sample can be expressed by

$$Q_3 = \Delta H_e W_3, \quad (3)$$

with $W_3 = W_1 + W_2$. Since the heat of fusion of the Bi(I) phase is known, the heat of fusion of the metastable phase can be determined from Eqs. (2) and (3) and the measured values of Q_1 , Q_2 , and Q_3 by

$$\Delta H_m = \Delta H_e Q_1 / (Q_3 - Q_2). \quad (4)$$

DSC thermograms for the measurement of the heat of fusion of the metastable phase are shown in Fig. 8. The value obtained was 5.98 kJ/g-at. The uncertainties involved in this

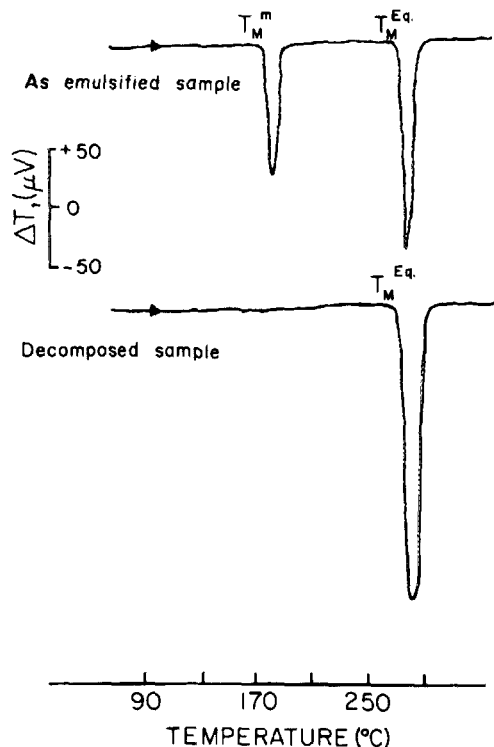


FIG. 8. DSC thermograms for a Bi droplet sample.

measurement are expected to be less than 10 % based upon repeated measurements.¹³

A perspective on the relative heat of fusion for Bi(II) compared to that for Bi(I) is provided in Fig. 9. Based on the measured heat capacity for the undercooled liquid¹³ the heat of fusion for Bi(I) at 447 K is almost twice the value for Bi(II). To extend the comparison to lower temperatures, the heat capacity of Bi(II) solid may be approximated with the value for Bi(I) solid as shown in Fig. 9.

Although the value for the heat of fusion of Bi(II) was not reported by Klement *et al.* so that the comparison is not possible, a value of 4.10 kJ/g-at. has been reported by Bridgman¹ at the Liquid-I-II triple point (1.7 GPa and 456 K).

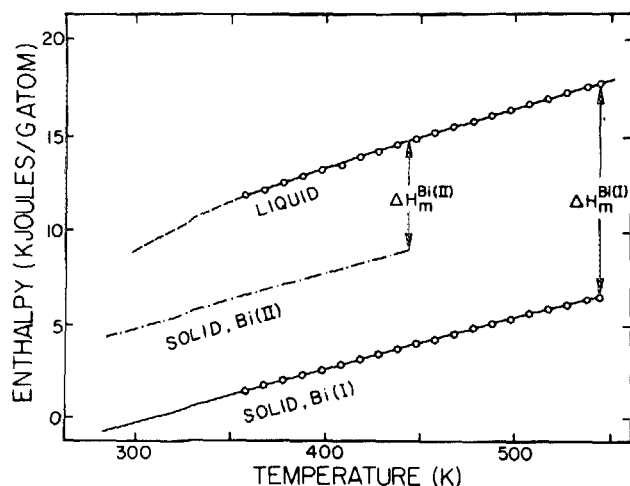


FIG. 9. Temperature dependence of the enthalpy for Bi(I), Bi(II), and liquid.

Moreover, if the heat of fusion of the Bi(II) is extrapolated linearly to 1 atm based on the data of the heat of transition of Bi(I) to Bi(II) and Bi(I) to liquid, the value is estimated to be about 6.90 kJ/g-at., which is within 10 % of the value measured in this work.

From the value of ΔH_m determined in this work and the Clausius-Clapeyron equation (Eq. 1), the ΔV value was calculated based on a gram volume of Bi(II) phase as 0.0013 cm³/g. Also, the volume per gram for Bi(II) at ambient pressure and 447 K is 0.0972 cm³/g. This value compares well with a neutron diffraction measurement⁴ of 0.0912 cm³/g at 2.6 GPa and room temperature.

According to the above thermodynamic or calorimetric evidence as well as the pressure results and the comparison with other high-pressure work, the metastable phase shown in the present Bi droplet sample is undoubtedly Bi(II), which solidified at deep undercooling. Similar observations of polymorphic phase formation during rapid solidification of undercooled liquids of antimony and gallium have been reported.¹⁴⁻¹⁷ In some cases the metastable structural modifications are known to correspond to those determined to be equilibrium structures at high pressure.

IV. DISCUSSION

The decomposition behavior of the metastable Bi(II) phase during cooling may be examined on the basis of the relevant free-energy relationships. In Fig. 10, the molar free energy of Bi is derived as a function of temperature from a combination of calorimetric measurements and published evaluations.¹⁸ It is apparent that a minimum undercooling of 97 °C is necessary before the metastable solid can form even under the most favorable heterogeneous nucleation kinetics. However, kinetic success in forming a metastable phase during initial nucleation will not necessarily allow for the most favorable conditions for retention of the structure in the sample. As noted in Fig. 10, the driving free-energy for decomposition of the metastable Bi(II) phase increases with decreasing temperature and appears to be a controlling factor for the decomposition during cooling after nucleation at maximum undercooling.

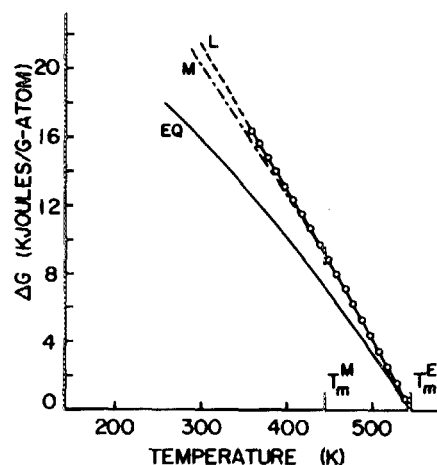


FIG. 10. Temperature dependence of molar free energy for different phases of pure Bi.

As mentioned above, the nucleation temperature of the sample that solidified at 56 °C, and atmospheric pressure decreases rapidly with pressure up to 100 MPa, but the pressure dependence becomes shallow with further increases of pressure. On the basis of classical nucleation theory¹⁹ and a structural model for the liquid-solid interface,²⁰ the trend of nucleation temperature of the sample to follow that of melting temperature of the sample on the P - T diagram can be rationalized.²¹ Therefore, the discontinuity of the pressure dependency of nucleation temperature around 100 MPa appears to be associated with the nucleation of the Bi(II) phase. That is, up to about 100 MPa, the majority of the droplets freeze as Bi(I) so that the trend of nucleation temperature follows that of the Bi(I) melting, which goes downward on P - T diagram. However, as pressure increases further, the portion of Bi(II) formed in the sample upon nucleation increases so that the trend of the nucleation temperature of the whole sample is affected by the increased portion of the Bi(II) in the sample. Since the nucleation temperature of the Bi(II) increases with pressure as the trend of the Bi(II) melting on P - T diagram over the present experimental pressure range, the nucleation temperature of the whole sample may be expected to increase with pressure over the range of 100–400 MPa. The nucleation temperature behavior of the sample solidified at 79 °C, which does not show a metastable endotherm throughout the experimental pressure range, and which shows a constant decrease of nucleation temperature as pressure increases supports this argument. A difference of dT_n/dP values between samples seems to come mainly from different potencies of heterogeneities in each sample and not from any capillarity-related pressure effects, which are more than an order of magnitude smaller in comparison to the experimental pressure range values.

A detailed analysis of the pressure dependence of nucleation temperatures for Bi- as well as Sn-emulsified samples will be presented elsewhere.²¹ However, it is important to note that even at the maximum undercooling which is equivalent to $0.41 T_m$, the nucleation behavior observed in the current work should not be viewed as representing homogeneous nucleation. The nature of the rate-controlling kinetics for either a volume-dependent or droplet-surface-dependent process requires the evaluation of careful nucleation rate measurements.¹⁹ Indeed, experience indicates that almost all undercooling values observed are limited by the onset of a heterogeneous nucleation process.

V. CONCLUSION

A metastable phase has been observed to nucleate in deeply undercooled Bi droplet samples. From the pressure dependence of the melting and nucleation behavior, and an assessment of the measured thermodynamic properties, the metastable phase has been identified as a high-pressure polymorph of Bi, i.e., Bi(II). This is an example, in which a high-pressure phase is solidified as a metastable phase in a rapid

solidification method. A trend of the pressure dependence of the nucleation temperature of droplet samples, which follows the trend of the melting temperature, has been observed and related to the development of competitive phase selection kinetics. It is noteworthy, however, that the pressure-induced transition in phase selection occurs at modest pressure levels so that the origin is certainly not due to a shift in relative thermodynamic stability of Bi(I) and Bi(II) under pressure, but rather to a change in the controlling nucleation kinetics.

ACKNOWLEDGMENTS

The authors are pleased to acknowledge support from the Army Research Office (DAAG29-80-K-0068 and DAAL03-86-K-0114). Special thanks are due to Dr. I. Anderson and C. Galaup. The assistance and hospitality of Professor C. A. Angell (Purdue University) during the early part of this work and Professor S. L. Cooper (University of Wisconsin-Madison) are gratefully acknowledged.

¹P. W. Bridgman, *Phys. Rev.* **48**, 893 (1935).

²C. G. Homan, *J. Phys. Chem. Solids* **36**, 1249 (1975).

³Powder Diffraction File, JCPDS, International Center for Diffraction Data (Swarthmore, PA, 1985), cards 5-519, 26-214.

⁴R. W. Brugger, R. B. Bennion, and T. G. Worlton, *Phys. Lett.* **24A**, 714 (1967).

⁵J. H. Perepezko and J. S. Paik, in *Proceedings of the 29th Midwest Solid State Conference: Novel Materials and Techniques in Condensed Matter*, edited by M. Blander, D. Karim, G. Crabtree, and P. Vashishta (North-Holland, New York, 1982).

⁶J. H. Perepezko and I. E. Anderson, in *Synthesis and Properties of Metastable Phases*, edited by T. J. Rowland and E. S. Machlin (TMS-AIME, Warrendale, PA, 1980), p. 31.

⁷D. Turnbull and R. E. Cech, *J. Appl. Phys.* **21**, 804 (1950).

⁸J. H. Perepezko, in *Rapid Solidification Processing: Principles and Technologies II*, edited by R. Mehrabian, B. H. Kear, and M. Cohen (Claitor's, Baton Rouge, LA, 1980), p. 56.

⁹J. H. Perepezko and J. S. Paik, in *Proceedings of the Materials Research Society Symposium: Rapidly Solidified Amorphous and Crystalline Alloys*, edited by B. H. Kear and B. C. Giessen (North-Holland, New York, 1982).

¹⁰J. H. Perepezko and J. S. Smith, *J. Non-Cryst. Solids* **44**, 65 (1981).

¹¹J. B. Yourtee and S. L. Cooper, *J. Appl. Polym. Sci.* **18**, 897 (1974).

¹²W. Klement, A. Jayaraman, and G. C. Kennedy, *Phys. Rev.* **131**, 632 (1963).

¹³J. H. Perepezko and J. S. Paik, *J. Non-Cryst. Solids* **61**, 113 (1984).

¹⁴L. Bosio, A. Defrain, and M. Dupont, *J. Chim. Phys.* **68**, 542 (1971).

¹⁵D. Akhtar, V. D. Vankar, T. C. Goel, and K. C. Chopra, *J. Mater. Sci.* **14**, 2422 (1979).

¹⁶J. H. Perepezko, C. Galaup, and K. P. Cooper, in *Proceedings of the Materials Research Society Symposium*, edited by G. E. Rindone (North-Holland, New York, 1982).

¹⁷J. A. Graves and J. H. Perepezko, *J. Mater. Sci.* (in press).

¹⁸R. Hultgren, P. D. Desai, D. T. Hawkins, M. Glesier, K. K. Kelly, and D. D. Wagman, *Selected Values of Thermodynamic Properties of the Elements* (American Society for Metals, Metals Park, OH, 1973).

¹⁹D. Turnbull, *J. Chem. Phys.* **20**, 411 (1952).

²⁰C. V. Thompson and F. Spaepen, *Acta Metall.* **31**, 2021 (1983).

²¹W. Yoon and J. H. Perepezko (unpublished).